CHAPTER 77

Nonsteady computations of undular and breaking bores

A.F.Teles da Silva [1] and D.H.Peregrine [2]

1. Introduction

A bore occurs when water with local depth h_1, say, moves over shallower water with depth h_2, necessarily moving at a lower speed, in a scale in which horizontal distances are a few times bigger than either h_1 or h_2. The bore is the region of transition between the two uniform depths and speeds. If the slopes are initially gentle, the bore gets gradually steeper and develops into one of three types depending on the ratio $\Delta = \frac{h_1 - h_2}{h_2}$. For small enough values of Δ, $\Delta <\simeq 0.3$, the bore front develops into a smooth succession of long waves. The difference between the upstream and downstream levels is fitted with undulations which are long at the front and short at the back. These are called undular bores. For big enough values of Δ, $\Delta >\simeq 0.7$, bore fronts break and the whole bore takes the aspect of a turbulent breaking zone extending over some depths and advancing at a constant speed (over a flat bed); outside this turbulent zone the water is flat. For intermediate values of Δ breaking and turbulence at the front precede a train of smooth undulations. Here the difference in level between upstream and downstream is fitted partially with breaking and turbulence in the front and partially with undulations. these bores are called undular breaking bores.

The classical bore theory, Lamb (1932) article 187, supposes a well developed bore advancing at constant speed and calculates the fluxes of mass, momentum and energy accross the bore in a frame of reference moving with the bore speed. It is shown that if mass and momentum are preserved, energy must be necessarily lost. Benjamin and Lighthill (1954), applied this approach, within the approximation of Kortweg & De Vries' equation, to the first

[1] Instituto de Matemática, Univ. Fed. do Rio de Janeiro & Lab. Mec. Fluidos, Prog. Eng. Mec., COPPE, CP68503, CEP21910, Rio de Janeiro - RJ, Brazil

[2] School of Maths, Univ. of Bristol, Bristol BS8 1TW, England

undulation of an undular bore; they show that, if mass momentum and energy are preserved, the wave is necessarily a solitary wave, if energy is lost the wave is a cnoidal wave. A limitation to the applicability of the classical approach to the whole of an undular bore is that, at any time, the flow at its back is unsteady; because new undulations are continualy forming and growing, turning the bore into an intrinsicaly unsteady phenomenon even if waves in the front assume a nearly steady aspect. Hence, in order to understand the bore as a whole, with its upstream and downstream regions, the evolution must be followed from an initial state. The simplest unsteady model is provided by shallow water equations; although, these are unable to predict undulations because vertical components of velocity are neglected. A higher order unsteady modelling is obtained by either Boussinesq's or Kortweg & De Vries' equations. Peregrine (1966), using a smooth transition as initial state, integrates Boussinesq's equations, numerically, in order to follow the evolution of gentle undular bores. The characteristic formation of smooth undulations is compared with the continuous steepening predicted by shallow water theory. Using K. & De V.'s equation, Gurevich & Pitaevskiĭ(1973), calculate analytically, an asymptotic solution valid for large values of time, the evolution of a step like initial condition. It is found that the separation between successive crests increases logaritmicaly and the height of the solitons at the head of the bore is 2Δ for an initial step of magnitude Δ.

In the present work we model the unsteady evolution of an initially gentle transition using a completely nonlinear mathematical formulation. The only approximations are the ones inherent to perfect fluid modelling. The flow is described by a potential of velocities ϕ which at any time obeys to:

$$\nabla^2\phi = 0 \tag{1}$$

$$\phi_t + \frac{1}{2}\nabla\phi^2 + gY = 0 \qquad\qquad \frac{D\mathbf{R}}{Dt} = \nabla\phi \tag{2}$$

$$\phi_y = 0 \tag{3}$$

$$\lim_{x\to-\infty} Y = h_1 - h_2 \qquad\qquad \lim_{x\to\infty} Y = 0$$

$$\lim_{x\to-\infty} \nabla\phi = (U_1, 0) \qquad\qquad \lim_{x\to\infty} \nabla\phi = (U_2, 0) \tag{4}$$

(1) is to be valid inside the fluid region; equations (2) are to be satisfied on the free surface which is described parametrically by $\mathbf{R} = (X, Y)$ to allow for overturning, g is the acceleration of gravity; equation (3) is valid on the flat bed placed at $y = -h_2$; the four

equations (4) are valid on the extremeties, $x = \pm\infty$ and h_1,h_2,U_1 and U_2 are given constants. Moreover we re scale distances by the downstream depth h_2 and accelerations by the acceleration of gravity g. The évolution of the free surface is calculated by a numerical method which is a modification of Dold & Peregrine's (1986) boundary integral scheme from the initial free surface profile

$$Y = \frac{\Delta}{2}[1 - tanh(\alpha X)] \tag{5}$$

For most of the computations the value of α has been set to $\alpha = 0.25$.

2. Numerical Results

Figure 1a shows the evolution of a strong bore, for $\Delta = 0.8$, for times 0, 2, 4, 6, 8, 10, 12 and 14, (from top to bottom in that order). Figure 1b shows the bore overturning at time 14.95. Figure 2a shows the evolution of an undular breaking bore, for $\Delta = 0.35$, for times 0, 10, 20, 30, 40, 60 and 70, with a vertical magnification of 10. This bore breaks at time 71.9; the breaking crest is shown in Figure 2b.

In order to assess the influence of Δ on the bore evolution we follow the growth of the first wave. Figure 3 shows graphs of height of the first crest, (x axis), against time, (y axis), for several values of Δ: 0.1, 0.2, 0.25, 0.28, 0.3, 0.3125, 0.325, 0.35, 0.4, 0.5, 0.6, 0.7, 0.8, 0.9, 1.0, 1.2 and 1.5 (from bottom to top). Waves have been followed until time 140, for cases in which breaking did not occur, and until the moment when a slope of 90^o first appear. Waves can, approximately, be grouped into three types:
i) the crest grows towards an asymptotic value;
ii) the crest first behaves as if in *i*) and then steeppens and rapidly breaks;
iii) the crest grows at an accelerated rate until breaking.
These typés correspond to the three bore types: undular, breaking and undular breaking. More details of the computations are given in Table 1. Table 1, below, gives the nondimensional time of breaking, t_b, which is the time when a slope of 90^o first appear, in $\sqrt{\frac{h_2}{g}}$ units; the height of breaking y_b; the horizontal distance travelled before breaking, x_b, in h_2 units. The front of the stronger bores break at a height that is slightly bigger than the original ($= \Delta$); also shown in Table 1 are H_1 and H_2 which are the distances from the first and second crests to the bed, respectively, divided by $1 + \Delta$, (upstream level); for Δ greater than 0.7, H_2 is nearly 1. meaning that secondary undulations almost cease to exist. As Δ grows beyond 1.5,

Figure 1a

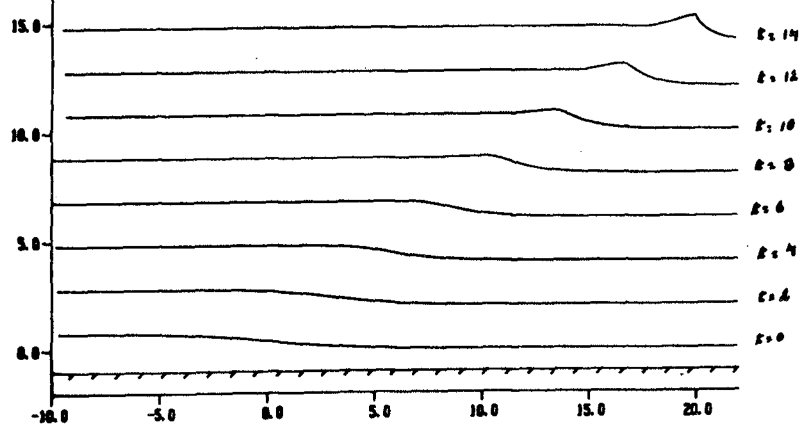

Figure 1b

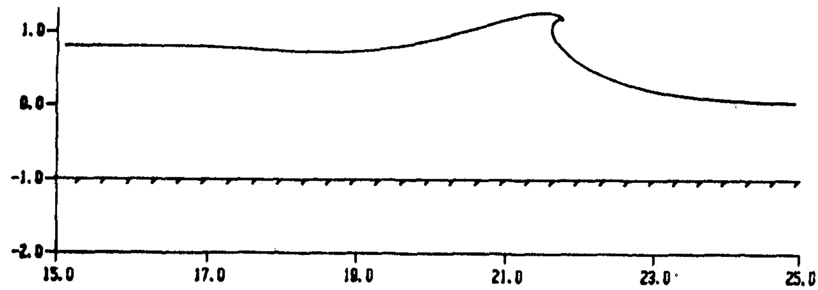

Figure 2a

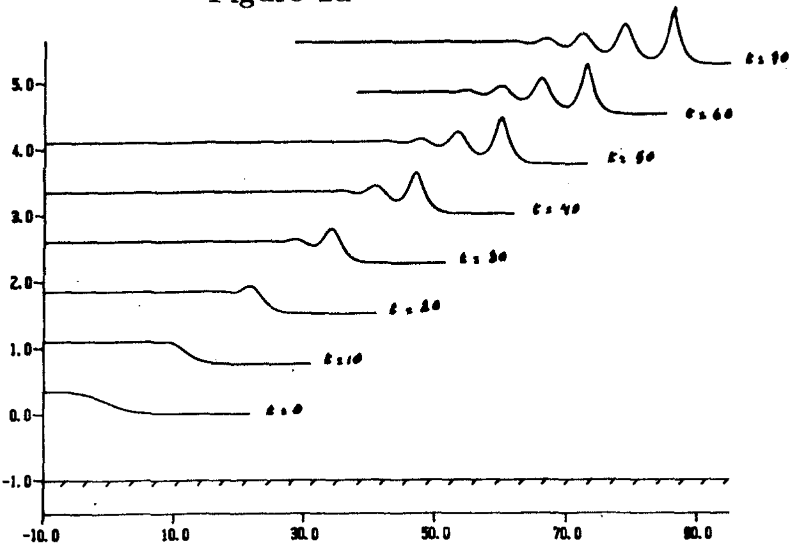

Figure 2b

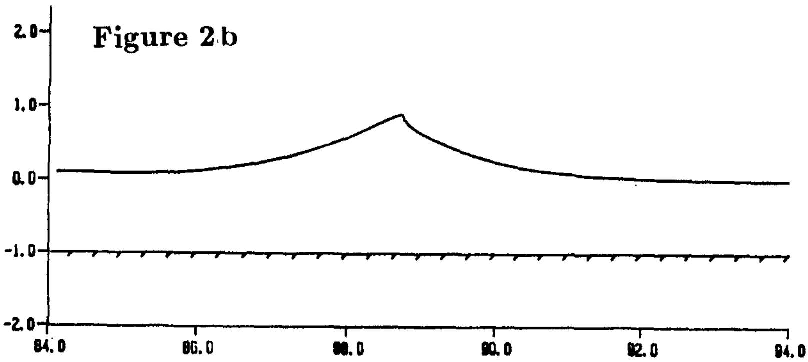

Figure 3

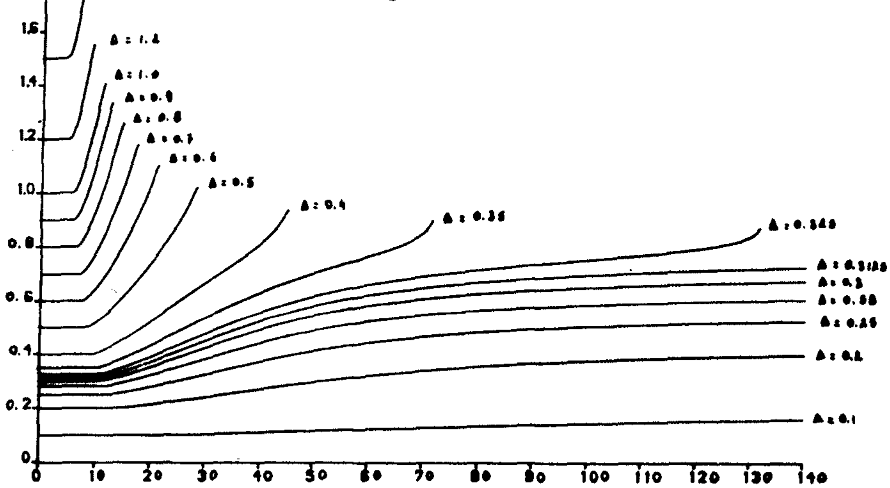

Figure 4

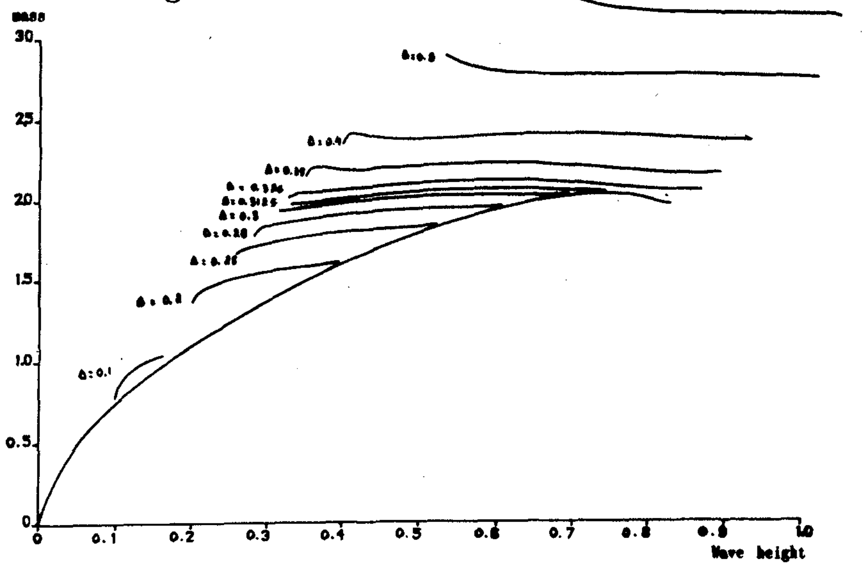

H_1 approaches 1.0; for higher values of Δ the bore breaks before a single wave forms; these facts also appear in the values of θ_1,θ_2, θ_3 and θ_4 which are respectively the maximum slopes, in degrees, of the front and back faces of the first and second waves. Note that after breaking the values of H_1 will be reduced.

Δ	t_b	x_b	y_b	H_1	H_2	θ_1	θ_2	θ_3	θ_4
0.325	131.7	164.4	0.87	1.42	1.28	81.5°	26.4°	11.9°	11.1°
0.35	71.9	88.7	0.89	1.40	1.19	88.5°	25.3°	4.3°	3.0°
0.4	45.3	56.2	0.93	1.40	1.12	84.9°	23.0°	1.2°	0.5°
0.5	28.3	36.3	1.02	1.35	1.05	83.5°	21.9°	0.0°	0.0°
0.6	21.1	28.0	1.10	1.31	1.03	85.7°	20.2°	0.0°	0.0°
0.7	17.1	23.5	1.18	1.28	1.00	84.8°	18.6°	0.0°	0.0°
0.8	14.4	20.5	1.26	1.25	1.00	86.2°	17.0°	0.0°	0.0°
1.0	11.1	17.0	1.41	1.20	1.00	84.2°	14.1°	0.0°	0.0°
1.2	9.2	15.0	1.55	1.16	1.00	89.5°	11.5°	0.0°	0.0°
1.5	7.4	13.1	1.77	1.11	1.00	85.5°	7.6°	0.0°	0.0°
2.0	-.-	-.-	-.-	1.05	1.00	87.2°	3.3°	0.0°	0.0°
3.0	-.-	-.-	-.-	1.03	1.00	91.8°	-.-°	0.0°	0.0°

Table 1

According to Benjamin and Lighthill (1954) the first wave of a well developed bore is a solitary wave. We expect the computed bores either to break or to develop into solitary waves. For this reason we compare properties of first waves in the bore with properties of solitary waves. Figure 4 shows graphs of mass of the first wave against wave-height for values of Δ equal to 0.1, 0.2, 0.25, 0.28, 0.3, 0.3125, 0.325, 0.35, 0.4, 0.5 and 0.6 (from bottom to top); also shown is the same relationship for the same range of solitary waves for comparison (the longer curve starting at the origin). Some remarkble facts can be observed: waves which are not going to break tend to assume the mass of a solitary wave even if wave-lengths at this stage, $t \leq 140.$, are all less than 4.5 depths; this fact have equally been observed for phase speed and maximum slope; waves which break have more mass than the maximum possible for solitary waves. Nonbreaking waves in Figure 4 tend to approach the solitary wave curve in a way that enables a rough estimate of asymptotic heights of undulations of nonbreaking bores. On this basis we conjecture that $\Delta \simeq 0.3$ is the highest limit for undular bores.

Another result about the evolution of bores is shown in Figure 5 where curves of wave-length of the first undulation is plotted against

Figure 5

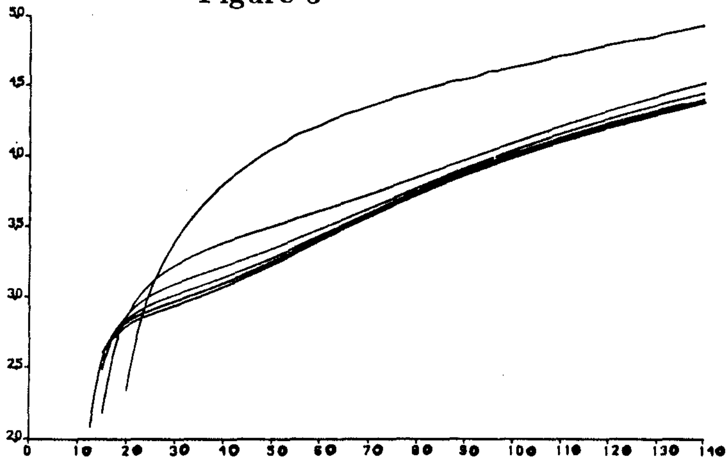

Figure 6

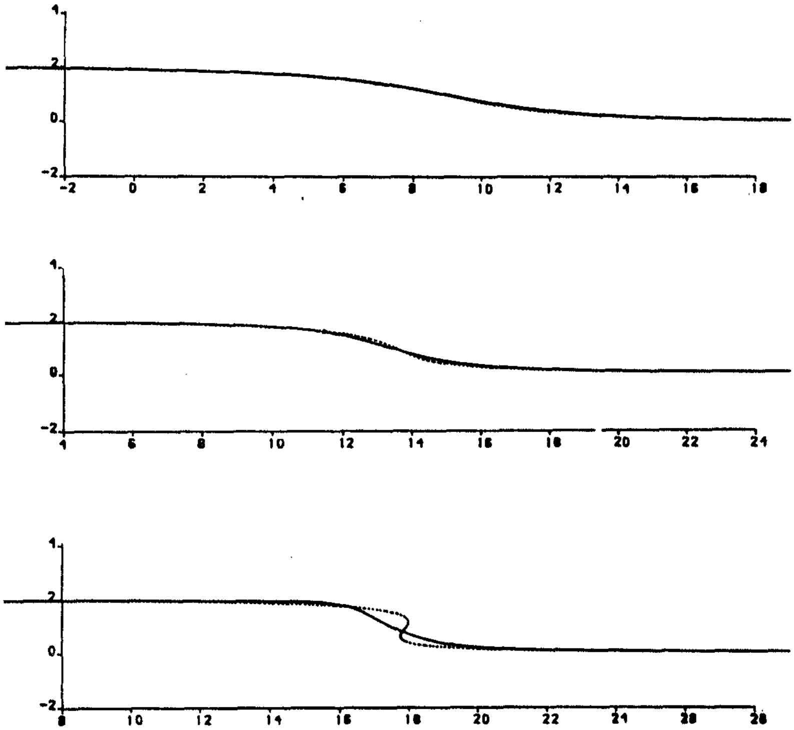

time; the wave-length of the first wave has been calculated as twice the horizontal distance from the crest to the trough just behind. A feature of Figure 5 that is important in the comparison with experiments is that bores undulations stretch faster for the gentler bores.

4. Comparison with weakly nonlinear results

In order to assess ranges of effectiveness of weakly nonlinear modelling we calculate the evolution of the initial free surface condition (5) using both shallow water and Boussinesq's equations and compare the results with the ones obtained by means of fully nonlinear calculations. Shallow water equations provide a good approximation for the initial stages of steepening of initially gentle bore fronts; for large values of Δ, where secondary undulations are not present, shallow water equations remain accurate for slopes up to $\simeq 20^o$. Boussinesq's equations are more suitable to model the initial stages of evolution of very small undulating bores. Figure 6 shows the comparison with shallow water equations for the initial condition (5) with $\alpha = 0.125$ and $\Delta = 2.0$; times shown are 4.0, 6.0, and 8.0 (from top to bottom).

There is a good agreement until time 6.0 when slopes are $\simeq 20^o$; after this point shallow water equations predict a too quick steepening and breaking.

Figure 7 shows a comparison between results from Boussinesq's equations (dashed lines) and full nonlinear computations (full lines) for $\alpha = 0.25$, time $= 50$ and $\Delta = 0.1$, 0.2 and 0.3 (from top to bottom). Boussinesq's equations overpredict undulation growth, bore speed and number of undulations in a way that errors increase with Δ and time for a fixed value of α.

5. Comparison with experiments

Favre (1935) conducts experiments in a canal $75.58m$ long and $0.41m$ wide; from Favre's experiments we are specialy interested in his first and third sets in which depth of water is $\simeq 0.2050m$ and $\simeq 0.1075m$, respectively. Results for $0.2050m$ of depth compares well with our computational experiments. In this set Δ varies from 0.062 to 0.278 depths. It is found that, at the end of the tank, after travelling for about 300 depths, the first waves acquire a nearly steady aspect; final wave-lengths range from $\lambda = 10.8$ depths to $\lambda = 8.6$ depths. Of special interest for comparisons are the bores with $\Delta = 0.202$ and $\Delta = 0.278$ depths which produce waves that at the end of the canal are respectively 0.395 and 0.570 depths of height. According to results in Figure 3 we can expect our calculated bores with $\Delta = 0.2$ and $\Delta = 0.28$ depths to produce solitary waves which are $\simeq 0.41$ and $\simeq 0.62$ depths high respectively. These figures

Figure 7

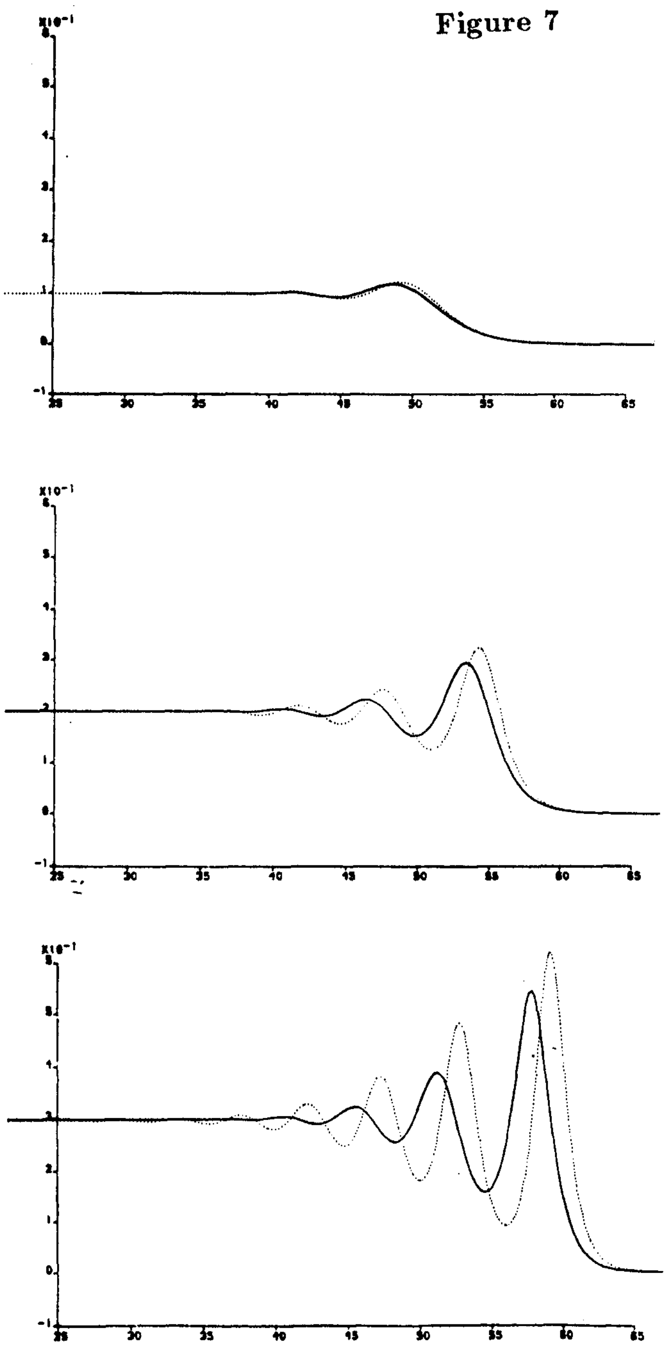

are respectively 3.8% and 8.8% higher than Favre's; the small differences can still be accounted for viscous dissipation of long waves travelling over long distances.

For depth $0.1075m$, Favre's third set, viscous effects are more conspicuous and results do not match as well with our calculations. In this set Δ ranges from 0.080 to 0.500 depths. One mismatch appears in the measured wave-lengths. In the previous set, undulations at the bore front for $\Delta = 0.238$ have a wave-length of 9.024 after travelling for about 300 depths; in depth $0.1075m$, with a bore with $\Delta = 0.230$, a wave-length of 8.47 depths is found at the end of the canal which is about 600 depths long. In a completely inviscid situation we should expect this later bore to attain greater wave-lengths for two reasons: gentler bores should stretch faster and bores continualy stretch as they travel further; (see Figure 5). The results of Figure 5 are confirmed by Favre's experiments of the same set. Another important difference between our inviscid results and Favre's third set is the breaking, spilling, of the bore front for $\Delta = 0.281$, at a distance of about 350 depths from the start of the canal; in his first set the bore with $\Delta = 0.278$ produces waves which are 0.570 depths high; one could expect smaller waves for $\Delta = 0.281$ because of a stronger viscous dissipation in shallower waters; this wave must break at a height smaller than 0.6 depths which is too small when compared with results for y_b in Table 1.

6. Bores on water of constant vorticity

Favre's results for depth $0.1075m$ are certainly more affected by viscosity than these for depth $0.2050m$. One of the effects of viscosity is dissipation of energy; but the sole dissipation of energy cannot be accounted for differences found in the comparison between inviscid results and Favre's experiments. Another important manifestation of viscosity, for long waves, is the shedding of vorticity generated at the boundary layer on the bed. Negative vorticity produced at the bed is difused into the fluid and its distribution varies with time and location which makes mathematical modelling a difficult task. For mathematical convenience we adopt a simple model in which vorticity is a constant. A perturbation in a 2D flow with constant vorticity can be represented by a potential flow. Hence, in order to introduce constant vorticity into the flow, we modify the boundary value problem for the potential ϕ given in equations (1) to (4) adding to the first and second equations (2), the terms:

$$-\omega(Y\phi_x - \psi)$$

to the left hand side of the first of equations (2), where ω is the value for the constant vorticity and ψ is a complex conjugate of ϕ

and

$$-\omega Y \mathbf{i}$$

to the right hand side of the second of equations (2).

Despite the simplicity of constant vorticity modelling, features of the third set of, depth = $0.1075m$, of Favre's experiments are present in our computations. Figure 8 shows the evolution of wave-length with time for irrotational and rotational bores: the full line curves are irrotational bores for $\Delta = 0.25$, upper curve, and $\Delta = 0.28$, lower curve; the dashed lines are rotational bores: for $\Delta = 0.28$ and $\omega = -0.125$, upper curve, and for $\Delta = 0.25$ and $\omega = -0.25$, lower curve. The two irrotational bores show the usual pattern in which the lower one is longer at any given time. Negative vorticity affects wave-lengths: the rotational bores are shorter than the corresponding irrotational ones, moreover the lower rotational bore, $\Delta = 0.25$ is made shorter by the use of stronger negative vorticity, $\omega = -0.25$ compared with $\omega = -0.125$. Another feature reproduced by constant negative vorticity modelling is breaking at smaller wave-heights; Figure 9 shows breaking of two bores with $\Delta = 0.8$, the dashed line bore is irrotational and the full line one moves in water of vorticity $\omega = -0.25$; the legend to the graph belongs to the rotational bore and the profile shown is for time 12. Results in Table 1 show that the corresponding irrotational bore breaks (with an angle of 90^o) at time 14.4 and its crest is, at the moment of breaking, at $x = 20.5$, hence negative vorticity causes premature breaking. About the profile of the bore $\Delta = 0.281$, Favre comments that it has the shape of a cycloid; such a comment cannot apply to irrotational waves. Figure 10 compares the profiles of the first two undulations of two bores, both with $\Delta = 0.25$; the one in dotted lines is an irrotational bore and the one in full lines represents the profile of a bore with vorticity $\omega = -0.25$. We notice that not only wave-lengths are shorter but crests are more peaked and troughs are flatter.

Positive vorticity has an opposite effect: Undulations tend to get longer, acquire a round sinusoidal shape and break at bigger heights when compared with irrotational ones. Bores which move up estuaries, probably, travel on water in which vorticity is mainly positive, generated by the boundary layer of the downstream river current. These bores should look rounder and move faster than bores running over still water.

7. Conclusions

Comparisons between Favre's first and third sets of experiments show that depth of water and width of the channel play an important role on results. Sandover and Zienckievicz (1957), conducted experiments on bores for channel depths of 2", 3", 4" and 6". They present

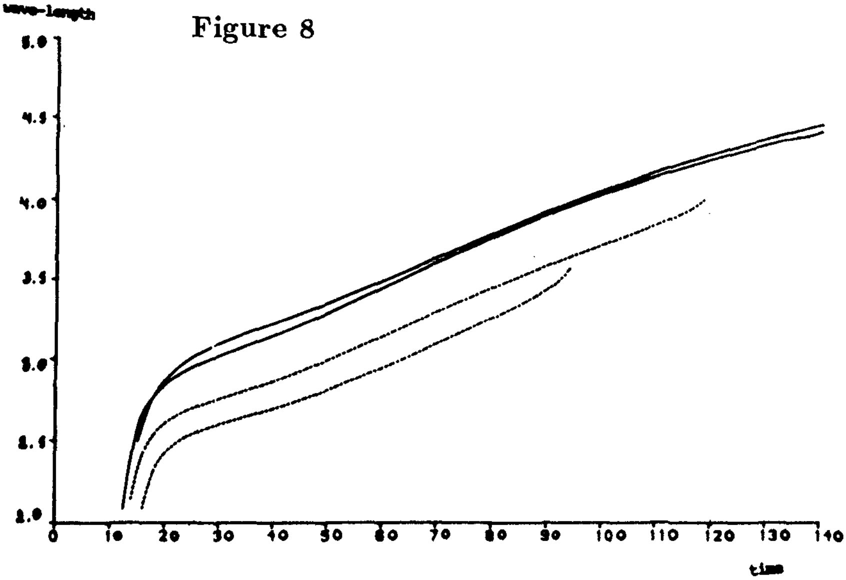
Figure 8
wave-length
time

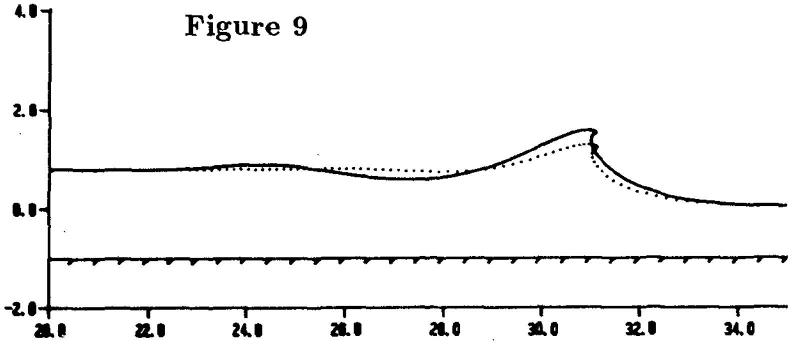
Figure 9

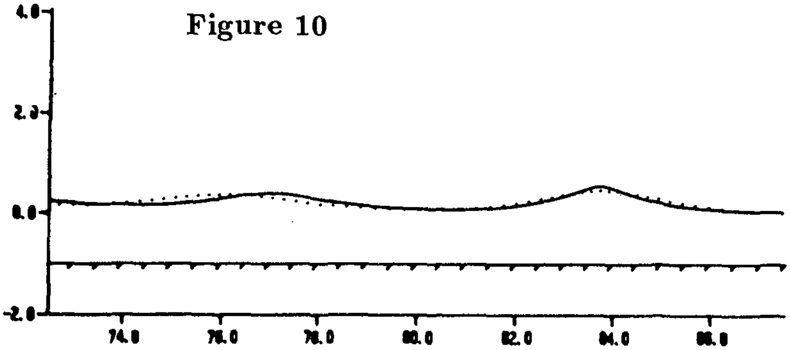
Figure 10

results for nondimensional discharge of water against wave-height at the end of the canal. These results show that for the same discharge wave-heights consistently increase with channel depth. They also show results for a channel in which the bed is rough and crests at the end of the canal are consistently lower when compared with results for the same discharge and depth on smooth beds.

Favre's and Sandover and Zienckievicz's results show that interaction with the boundary layer at the bed may be important in the analysis of results of experiments with bores. The presence of a boundary layer has two important effects: dissipation of energy and generation of vorticity. Dissipation of energy contributes to lower wave heihts and the presence of vorticity will have an effect on breaking, on wave-lengths, on wave shape and on the limit on maximum Δ for undular bores.

Results in Figure 4 and Table 1 lead to the conclusion that maximum height of bores divided by upstream depth, H_1, grows with Δ for $\Delta <\simeq 0.3$ and then decay for breaking bores, ($\Delta >\simeq 0.3$). The limiting figures 0.3 and 0.7 have been found through an irrotational modelling; how this figures will change in real situations may depend on average values of vorticity. In situations in which vorticity is negative, as it happens in bores running over still water, the only vorticity is produced at the bed by the undulations, these figures will be smaller. In situations in which the bore moves upstream a current, the average vorticity can be positive and the limiting waves higher.

8. References

Benjamin, T. B. & Lighthill, M. J. (1954)
On cnoidal waves and bores. Proc. Roy. Soc. A, 224, 448-460.

Dold, J. W. & Peregrine, D. H. (1986)
An efficient boundary int. meth. for steep unsteady waves. Numerical methods for fluid dynamics II, eds: K. W. Morton & M. J. Baines, pp 671-679. Clarendon Press, Oxford.

Favre, H. (1935)
Etude théor. et expérimental des ondes de translation. Dunod, Paris.

Gurevich, A. V. & Pitaevskiĭ, L. P. (1973)
Nonstationary structure of a colisionless shock wave. Zh. Eksp. Theor. Fiz. 65, 590-604

Lamb, H. (1932)
Hydrodynamics. Dover, New York.